A Passive Localization Algorithm and Its Accuracy Analysis

BENJAMIN FRIEDLANDER, FELLOW, IEEE

(Invited Paper)

Abstract—**The problem of estimating source location from noisy measurements of range differences (RD's) is considered. A localization technique based on solving a set of *linear* equations is presented and its accuracy properties are analyzed. An optimal weighting matrix for the least squares estimator is derived. The analytical expressions for the variance and bias of the estimator are validated by Monte-Carlo simulation. The problem of estimating source velocity given measurements of range differences and range-rate differences is briefly considered, and a linear equation technique is derived.**

I. Introduction

A common method for localizing an acoustic or electromagnetic source is based on measuring the range differences to several points whose locations are known. In various navigation systems (e.g., Loran, Decca, Omega) the measurement consists of observing differences in the time of arrival of signals from sources at known locations to a receiver at the unknown location. In the passive sonar problem, signals travel from a source whose location is to be estimated to sensors whose positions are known.

The conventional approach to estimating source location is based on finding the hyperbolic lines of position (LOP's); see [9]–[11]. Each range (or time) difference determines a hyperbola,[1] and the point at which these hyperbolas intersect is the estimated source location (see Fig. 1).

The hyperbolic LOP approach has several serious drawbacks: the computation of the intersection location is quite cumbersome; these solutions do not appear to be easily extended to other situations such as calculating source velocity from range differences and their rates of change (cf. Section V). Furthermore, the complexity of the solutions makes error analysis very difficult.

An alternative approach, which circumvents many of these difficulties, was proposed in [1]. This approach is based on the idea that three sensors with their set of range differences determine a straight line of position. In fact, this line is the major axis of a general conic which passes through the sensors. When more than three sensors are available, several straight LOP's are generated and their intersection provides an estimate of the source location (see Fig. 2).

Manuscript received May 5, 1986; revised September 5, 1986. This work was supported in part by the Office of Naval Research under Contract N00014-87-C-0147.

The author is with Saxpy Computer Corp., Sunnyvale, CA 94086.

IEEE Log Number 8714343.

[1] We are considering here the two-dimensional case, i.e., the source and sensors are located in a plane.

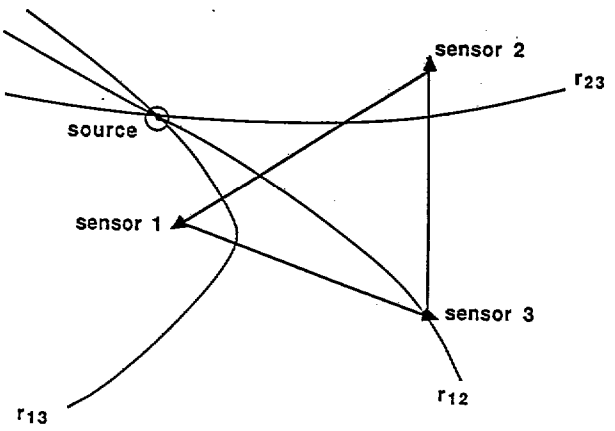

Fig. 1. Hyperbolic lines of position.

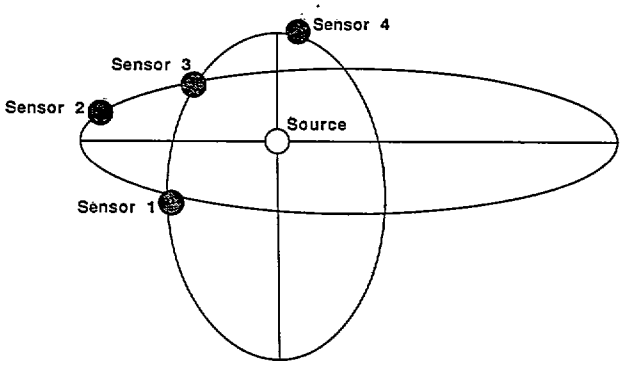

Fig. 2. Location on the conic axis.

The method proposed in [1] computed the intersection point from a set of $\binom{N}{3} \triangleq (N!/(N-3)!3!)$ linear equations, N being the number of sensors. This approach alleviates some of the difficulties of the hyperbolic LOP method. However, it introduces some inconsistencies due to its use of redundant information: this problem formulation leads to a set of $\binom{N}{3}$ equations while, in fact, there are only N available measurements (see [2] for a more detailed discussion).

A different formulation is proposed in [2] and [3] based on the straight LOP approach, which leads to a set of N equations. This set of equations contains all the relevant sensor data without redundancy. However, due to a nonlinear relationship between certain variables in these equations, the location can no longer be computed by a linear estimation procedure. An iterative gradient search procedure is proposed in [3] to compute the the source location.

0364-9059/87/0100-0234$01.00

Subtracting one of the equations in [2] and [3] from the $(N-1)$ remaining equations leads to a set of $(N-1)$ equations containing a single nonlinear term. It was recently noted in [4] that this nonlinearity can be eliminated by a two-step least squares procedure to yield a closed-form expression for the source location. This noniterative technique appears to be very attractive both in its modest computational requirements and its performance.

In this paper we present a localization technique based on the solution of a set of either $(N-1)$ or $(N-2)$ linear equations. While the derivation and resulting solution appear different from the one in [4], it is shown that the two are mathematically equivalent. However, the method presented here is somewhat simpler and reveals more clearly the underlying structure of the solution.

The main contribution of this paper is in providing an accuracy analysis of the proposed solution method. In Section III we derive approximate expressions for the bias and variance of the location estimates. The variance formula is used to derive an optimal weighting matrix for the least squares location estimator. In Section VI we verify these formulas by Monte-Carlo simulations.

The methods presented in [1]–[4] and in Section II all require that the number of sensors N be greater than $(n+1)$ where n is the dimension of the space in which the sensors and source are located (in other words, $N > 3$ in the two-dimensional case and $N > 4$ in the three-dimensional case). In some practical situations no more than $N = n+1$ sensors are available. In Section IV we derive explicit expressions for the source location for this case. These expressions are somewhat more complicated than the one for $N > n+1$, and their accuracy is not analyzed here.

In some situations, it is possible to measure both the range differences and the range-rate differences (e.g., by measuring Doppler shifts of spectral lines). Using these measurements it is possible to estimate source velocity as well as source location. A linear equation technique for estimating source velocity is presented in Section V. In Section VII we discuss some additional applications of the results derived in this paper.

II. Localization from Range Differences

In this section we state and solve the localization problem for the three-dimensional case. The discussion here and in the following sections will be in terms of range difference measurements. However, the same results apply to localization from delay difference measurements. Delay can be converted into range simply by multiplying it by the speed of propagation.

Let $\boldsymbol{x}_i = [x_i, y_i, z_i]^T$ denote the (x, y, z) coordinates of the ith sensor and $\boldsymbol{x}_s = [x_s, y_s, z_s]$ denote the source coordinates. The distance between the source and the ith sensor is $R_{is} \triangleq \|\boldsymbol{x}_i - \boldsymbol{x}_s\|$. The distance from the origin to the ith sensor is $R_{io} \triangleq \|\boldsymbol{x}_i\|$, and the distance to the source is $R_{so} = \|\boldsymbol{x}_s\|$. Let r_{ij} be the range difference (RD) for sensors i and j where

$$r_{ij} = R_{is} - R_{js} = \|\boldsymbol{x}_i - \boldsymbol{x}_s\| - \|\boldsymbol{x}_j - \boldsymbol{x}_s\|. \tag{1}$$

The various quantities defined above are depicted in Fig. 3.

The localization problem is to estimate $\boldsymbol{x}_s$ given noise measurements of the RD's $\{r_{ij}, i, j = 1, \cdots, N\}$ provided by N sensors. Note that there are $\binom{N}{2} = (N(N-1)/2)$ distinct RD's. However, all of these RD's can be completely determined from only $(N-1)$ RD's (e.g., $\{r_{i1}, i = 2, \cdots, N\}$) in the noiseless case.

Using the notation above, we can derive the basic equations in a straightforward manner. Note that

$$R_{is}^2 = (r_{ij} + R_{js})^2 = r_{ij}^2 + 2R_{js}r_{ij} + R_{js}^2 \tag{2}$$

and also that

$$R_{is}^2 = \|\boldsymbol{x}_i - \boldsymbol{x}_s\|^2 = R_{io}^2 - 2\boldsymbol{x}_i^T\boldsymbol{x}_s + R_{so}^2. \tag{3}$$

Subtracting (3) from (2) and rearranging terms, we get

$$2\boldsymbol{x}_i^T\boldsymbol{x}_s = R_{io}^2 - r_{ij}^2 - 2R_{js}r_{ij} + R_{so}^2 - R_{js}^2. \tag{4}$$

Setting $i = j$ in (4) gives

$$2\boldsymbol{x}_j^T\boldsymbol{x}_s = R_{jo}^2 + R_{so}^2 - R_{js}^2 \tag{5}$$

where we used the fact that $r_{jj} = 0$. Subtracting (5) from (4) yields

$$2(\boldsymbol{x}_i - \boldsymbol{x}_j)^T\boldsymbol{x}_s = (R_{io}^2 - R_{jo}^2) - r_{ij}^2 - 2R_{js}r_{ij} \tag{6}$$

which can be written in matrix form as

$$S_j\boldsymbol{x}_s = \boldsymbol{\mu}_j - R_{js}\boldsymbol{\rho}_j \tag{7a}$$

where

$$S_j = \begin{bmatrix} (x_1 - x_j) & (y_1 - y_j) & (z_1 - z_j) \\ \vdots & \vdots & \vdots \\ (x_{j-1} - x_j) & (y_{j-1} - y_j) & (z_{j-1} - z_j) \\ (x_{j+1} - x_j) & (y_{j+1} - y_j) & (z_{j+1} - z_j) \\ \vdots & \vdots & \vdots \\ (x_N - x_j) & (y_N - y_j) & (z_N - z_j) \end{bmatrix}, \quad (N-1)\times 3 \tag{7b}$$

$$\boldsymbol{\mu}_j = \frac{1}{2} \cdot \begin{bmatrix} R_{1o}^2 & -R_{jo}^2 & -r_{1j}^2 \\ \vdots & \vdots & \vdots \\ R_{j-1o}^2 & -R_{jo}^2 & -r_{j-1j} \\ R_{j+1o}^2 & -R_{jo}^2 & -r_{j+1j} \\ \vdots & \vdots & \vdots \\ R_{No}^2 & -R_{jo}^2 & -r_{Nj} \end{bmatrix}, \quad (N-1)\times 1 \tag{7c}$$

$$\boldsymbol{\rho}_j = \begin{bmatrix} r_{1j} \\ \vdots \\ r_{j-1j} \\ r_{j+1j} \\ \vdots \\ r_{Nj} \end{bmatrix}, \quad (N-1)\times 1. \tag{7d}$$

The reference sensor j can be chosen to be any one of the N sensors. We will comment on this further in Section VI.

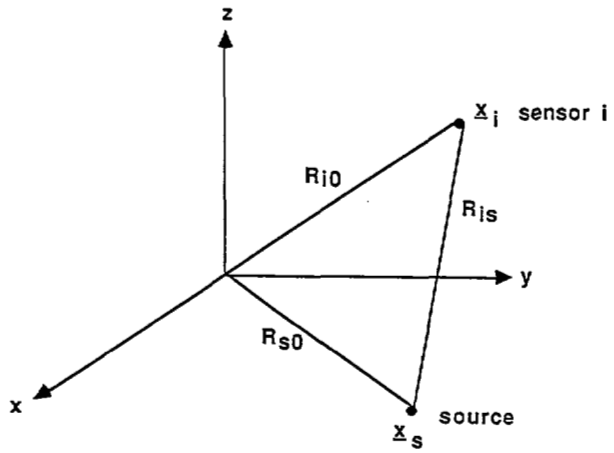

Fig. 3. Sensor-source geometry.

Note that given the measurements $\{r_{ij}, i = 1, \cdots, N\}$, the vectors μ_j, ρ_j are known; so is the matrix S_j, which depends only on the sensor locations (assumed to be known). The unknown quantities in (7a)–(7d) are the location vectors x_s and the distance R_{js} between the source and the reference sensor, which is a function of (the unknown) x_s. It is the presence of R_{js} that complicates the solution of (7).

Our approach is based on the idea of eliminating the "nuisance parameter" R_{js} by premultiplying (7a) by a matrix M which has ρ_j in its null-space, i.e., $M\rho_j = 0$. The matrix

$$M_j^{(k)} = (I - Z^k)D_j \tag{8a}$$

where

$$D_j = [\text{diag } \{\rho_j\}]^{-1} = \begin{bmatrix} r_{ij} & & & & 0 \\ & \ddots & & & \\ & & r_{j-1\,j} & & \\ & & & r_{j+1\,j} & \\ & & & & \ddots \\ 0 & & & & r_{Nj} \end{bmatrix}^{-1} \tag{8b}$$

$$Z = \begin{bmatrix} 0 & 1 & & 0 \\ & \ddots & \ddots & \\ & 0 & \ddots & 1 \\ 1 & & & 0 \end{bmatrix} = \text{circular shift matrix} \tag{8c}$$

clearly has this property for any value of k, since

$$D_j\rho_j = \mathbf{1} \triangleq [1, 1, \cdots, 1]^T \tag{9}$$

and

$$(I - Z^k)\mathbf{1} = \mathbf{1} - Z^k\mathbf{1} = \mathbf{1} - \mathbf{1} = 0. \tag{10}$$

To simplify the subsequent discussion, we assume that $k = 1$ and suppress the superscript in $M_j^{(k)}$. From the property of M_j discussed above, it follows that

$$M_jS_jx_s = M_j\mu_j. \tag{11}$$

The location vector x_s can now be computed by using any good least squares equation solver on the *linear* set of (11), see for example [5] and [6]. A closed-form solution which is useful for some subsequent derivations is given by

$$x_s = (S_j^TM_j^TM_jS_j)^{-1}S_j^TM_j^TM_j\mu_j. \tag{12}$$

It should be noted that M_j is a singular matrix of rank $N - 2$. For M_jS_j to be nonsingular it is necessary (although not sufficient) that the number of rows of S_j be larger than the number of columns, i.e., $N - 1 \geq n$ (where n is the dimension of x_s). Thus, for a unique solution of (11) to exist, we must have $N > n + 1$. The case $N = n + 1$ will be discussed later.

The approach taken in [4] is based on a two-step procedure. First it is assumed that R_{js} is known, in which case a least squares solution for x_s is given by

$$x_s = (S_j^TS_j)^{-1}S_j^T(\mu_j - R_{js}\rho_j). \tag{13}$$

Next R_{js} is chosen to minimize $\|S_jx_s - (\mu_j - R_{sj}\rho_j)\|^2$ or equivalently $\|P_j(\mu_j - R_{sj}\rho_j)\|^2$ where

$$P_j = I - S_j(S_j^TS_j)^{-1}S_j. \tag{14}$$

It is straightforward to show that the minimizing R_{sj} is given by

$$R_{sj}^* = \frac{\rho_j^TP_j\mu_j}{\rho_j^TP_j\rho_j}. \tag{15}$$

Thus the method presented in [4] computes the location vector by the least squares solution of

$$S_jx_s = \left(\mu_j - \frac{\rho_j^TP_j\mu_j}{\rho_j^TP_j\rho_j}\rho_j\right). \tag{16}$$

Let us denote the solution obtained from (11) x_s^1 and from (16) x_s^2. Note that

$$M_jS_jx_s^2 = M_j\mu_j = M_jS_jx_s^1 \tag{17}$$

or

$$M_jS_j(x_s^1 - x_s^2) = 0.$$

Since M_jS_j is assumed to be nonsingular, it follows that $x_s^1 = x_s^2$. Establishing this fact by algebraic manipulation of (11) and (16) is quite cumbersome.

An Alternative Form of (11)

In the following section we will find it convenient to use a slightly different form of the location estimator. Note that the matrix $(I - Z^k)$ [cf. (8a)] is an $(N - 1) \times (N - 1)$ matrix with rank $(N - 2)$. Thus the singular value decomposition (SVD) of this matrix will have the form

$$(I - Z^k) = [U_k, u_k] \begin{bmatrix} \eta_1^k & & 0 \\ & \ddots & \\ 0 & & \eta_{N-2}^k \\ & & 0 \end{bmatrix} [V_k, v_k]^T$$

$$= U_k \text{ diag } \{\eta_1^k, \cdots, \eta_{N-2}^k\} V_k^T \tag{18}$$

where U_k, V_k are $(N-1) \times (N-2)$ orthogonal matrices and $\{\eta_1^k, \cdots, \eta_{N-2}^k\}$ are the $(N-2)$ nonzero singular values of $(I - Z^k)$. Since $(I - Z^k)\mathbf{1} = 0$, it follows that $V_k^T\mathbf{1} = 0$. Therefore, another candidate for the matrix M_j which was used to "annihilate" the second term in (7a) is

$$\bar{M}_j = V_k^T D_j. \tag{19}$$

Premultiplying (7a) by this matrix leads to a set of $(N-2)$ linear equations for $\boldsymbol{x}_s$

$$\bar{M}_j S_j \boldsymbol{x}_s = \bar{M}_j \boldsymbol{\mu}_j \tag{20}$$

whereas (11) consisted of $(N-1)$ linear equations. In the following we will suppress the subscript k in V_k.

III. Accuracy Analysis of the Location Estimate

In the discussion so far we assumed the availability of perfect measurements $\{r_{ij}\}$. In this section we analyze the effect of noise on the location estimates. We assume that the RD's are corrupted by additive mutually uncorrelated zero-mean white Gaussian noise with covariance matrix

$$\Sigma = \text{diag}\,\{\sigma^2\}, \qquad \sigma^2 = [\sigma_1^2, \sigma_2^2, \cdots, \sigma_{N-1}^2]^T. \tag{21}$$

The measured RD's are denoted $\hat{\boldsymbol{\rho}}_j$ and

$$\hat{\boldsymbol{\rho}}_j = \boldsymbol{\rho}_j + \boldsymbol{n}_j \tag{22}$$

where $\boldsymbol{n}_j \sim \mathfrak{N}(0, \Sigma)$. The location vector obtained when $\hat{\boldsymbol{\rho}}_j$ is used instead of $\boldsymbol{\rho}_j$ is denoted $\hat{\boldsymbol{x}}_s$, where $\hat{\boldsymbol{x}}_s = \boldsymbol{x}_s + \tilde{\boldsymbol{x}}_s$, $\tilde{\boldsymbol{x}}_s$ being the error vector. Similarly, we denote $\hat{R}_{js} = \|\boldsymbol{x}_j - \hat{\boldsymbol{x}}_s\|$ and $\hat{r}_{js} = R_{js} + R_{js}$, where $\tilde{R}_{js}$ is the error term.

Inserting $\hat{\boldsymbol{x}}_s$, $\hat{\boldsymbol{\rho}}_j$, and $\hat{R}_{js}$ into (7a) we get

$$S_j\hat{\boldsymbol{x}}_s = S_j\boldsymbol{x}_s + S_j\tilde{\boldsymbol{x}}_s = \left(\boldsymbol{\mu}_j - \boldsymbol{\rho}_j \odot \boldsymbol{n}_j + \tilde{R}_{js}\boldsymbol{\rho}_j + \frac{1}{2}\boldsymbol{n}_j \odot \boldsymbol{n}_j + \tilde{R}_{js}\boldsymbol{n}_j\right) \tag{23}$$

where $\odot$ denotes element-by-element multiplication of two vectors. Alternatively

$$S_j\tilde{\boldsymbol{x}}_s = -\left[(\boldsymbol{\rho}_j + R_{js}\mathbf{1}) \odot \boldsymbol{n}_j + \tilde{R}_{js}\boldsymbol{\rho}_j + \frac{1}{2}\boldsymbol{n}_j \odot \boldsymbol{n}_j + \tilde{R}_{js}\boldsymbol{n}_j\right]. \tag{24}$$

or

$$\text{COV}\,\{\tilde{\boldsymbol{x}}_s\} = F_j \Sigma F_j^T \tag{27a}$$

where

$$F_j = (S_j^T M_j^T M_j S_j)^{-1} S_j^T M_j^T M_j\,(\text{diag}\,\{\boldsymbol{\rho}_j\} + R_{js}I). \tag{27b}$$

It should be noted that by performing a first-order Taylor-series expansion of $\hat{\boldsymbol{x}}_s$ around $\boldsymbol{x}_s$ it follows that F_j is the matrix of the first derivatives of $\hat{\boldsymbol{x}}_s$ with respect to the measurements $\{r_{ij}\}$, i.e., $F_j = (\partial\hat{\boldsymbol{x}}_s/\partial\boldsymbol{\rho}_j)$. Thus (27) can be derived by differentiating (11).

The derivation of the bias can be done by a second-order Taylor-series expansion of $\hat{\boldsymbol{x}}_s$. It is straightforward to show that

$$E\{\tilde{x}_s\} = E\left\{\boldsymbol{n}_j^T \frac{\partial^2 x_s}{\partial\boldsymbol{\rho}_j^2}\boldsymbol{n}_j\right\} = \text{tr}\left\{\text{diag}\left\{\frac{\partial^2 x_s}{\partial\boldsymbol{\rho}_j^2}\right\}\Sigma\right\}$$

and similarly

$$E\{\tilde{y}_s\} = \text{tr}\left\{\text{diag}\left\{\frac{\partial^2 y_s}{\partial\boldsymbol{\rho}_j^2}\right\}\Sigma\right\}.$$

The second-order derivative matrices of x_s and y_s are somewhat complicated (cf. [12]) and will not be presented here. Instead we will consider two approximate formulas which are simpler than the "exact" formula and yet provide satisfactory results in many cases.

The first derivation involves approximating the noisy version of M_j (i.e., M_j computed using noisy range differences) by the true M_j. We then take the expected value of both sides of (24) and premultiply by M_j to get

$$M_j S_j E\{\tilde{\boldsymbol{x}}_s\} = -M_j\left[E\left\{\frac{1}{2}\boldsymbol{n}_j \odot \boldsymbol{n}_j\right\} + E\{\tilde{R}_{js}\boldsymbol{n}_j\}\right]. \tag{28}$$

Note that in this case we do not neglect the last two terms of (24). In fact, it is precisely these terms that introduce the bias. The multiplication by M_j is necessary to eliminate the term $E\{\tilde{R}_{js}\}\boldsymbol{\rho}_j$.

The first term is the square brackets above is simply σ^2. To evaluate the second term we insert $\hat{\boldsymbol{\rho}}_j$ into (15) to obtain (after reordering of terms)

$$\tilde{R}_{js} = \frac{\boldsymbol{\rho}_j^T P_{jj}\boldsymbol{\mu}_j - \boldsymbol{\rho}_j^T P_j\boldsymbol{\rho}_j \odot \boldsymbol{n}_j - \boldsymbol{\mu}_j^T P_j\boldsymbol{n}_j - \boldsymbol{\rho}_j^T P_j\boldsymbol{n}_j \odot \boldsymbol{n}_j - \frac{1}{2}\boldsymbol{\rho}_j^T P_j\boldsymbol{n}_j \odot \boldsymbol{n}_j - \frac{1}{2}\boldsymbol{n}_j^T P_j\boldsymbol{n}_j \odot \boldsymbol{n}_j}{\boldsymbol{\rho}_j^T P_j\boldsymbol{\rho}_j + 2\boldsymbol{\rho}_j^T P_j\boldsymbol{n}_j + \boldsymbol{n}_j^T P_j\boldsymbol{n}_j}. \tag{29}$$

To evaluate the covariance matrix of $\tilde{\boldsymbol{x}}_s$ we make some approximations. Assuming small error conditions, we will neglect any terms which contain products of errors. Thus the two last terms in (24) are neglected. Next note that

$$M_j S_j\tilde{\boldsymbol{x}}_s \cong -M_j(\boldsymbol{\rho}_j + R_{js}\mathbf{1}) \odot \boldsymbol{n}_j \tag{25}$$

from which it readily follows that

$$M_j S_j\,\text{COV}\,\{\tilde{\boldsymbol{x}}_s\} S_j^T M_j^T = M_j\,(\text{diag}\,\{\boldsymbol{\rho}_j\} + R_{js}I)\Sigma\,(\text{diag}\,\{\boldsymbol{\rho}_j\} + R_{js}I)M_j^T \tag{26}$$

To evaluate $\tilde{R}_{sj}$ we will make a small error approximation and neglect all terms containing products of noise variables (i.e., the last three terms in the numerator and the last term in the denominator). Next we use the standard approximation

$$\frac{1}{\boldsymbol{\rho}_j^T P_j\boldsymbol{\rho}_j + 2\boldsymbol{\rho}_j^T P_j\boldsymbol{n}_j} \cong \frac{1}{\boldsymbol{\rho}_j^T P_j\boldsymbol{\rho}_j}\left(1 - 2\frac{\boldsymbol{\rho}_j^T P_j\boldsymbol{n}_j}{\boldsymbol{\rho}_j^T P_j\boldsymbol{\rho}_j}\right) \tag{30}$$

to get

$$\tilde{R}_{js} \cong -\frac{1}{\boldsymbol{\rho}_j^T P_j\boldsymbol{\rho}_j}[\boldsymbol{\rho}_j^T P_j\boldsymbol{\rho}_j \odot \boldsymbol{n}_j + (2R_{js}\boldsymbol{\rho}_j^T - \boldsymbol{\mu}_j^T)P_j\boldsymbol{n}_j]. \tag{31}$$

Note that

$$P_j(\mu_j - R_{js}\rho_j) = P_j(S_j x_s) = 0 \tag{32}$$

and therefore the second term in (31) reduces to $-R_{js}\rho_j^T n_j$. It follows that

$$E\{\tilde{R}_{js} n_j\} = -\frac{1}{\rho_j^T P_j \rho_j} \cdot [R_{js} P_j \rho_j + \text{diag}\,\{\rho_j\} P_j \rho_j] \odot \sigma^2 \triangleq \delta_j. \tag{33}$$

Inserting (33) in (28) we get

$$M_j S_j E\{\tilde{x}_s\} = -M_j \left(\frac{1}{2}\sigma^2 + \delta_j\right) \tag{34}$$

or

$$\text{BIAS} = E\{\tilde{x}_s\} = -(S_j^T M_j^T M_j S_j)^{-1} S_j^T M_j^T M_j \left(\frac{1}{2}\sigma^2 + \delta_j\right). \tag{35}$$

Next we derive a formula for the bias which takes into account the fact that the M_j used in (11) is corrupted by the measurements noise.

From (22) and (8) it follows that

$$\hat{M}_j \triangleq Z\hat{D}_j = Z\,(\text{diag}\,\{\rho_j\} + N_i)^{-1} = ZD_j(I + D_j N_j)^{-1} \tag{36}$$

where $N_j \triangleq \text{diag}\,\{n_j\}$.

Using the approximation $(I + X)^{-1} \cong I - X$ we get

$$\hat{M}_j \cong M_j(I - D_j N_j). \tag{37}$$

Next note that

$$\hat{M}_j^T \hat{M}_j = M_j^T M_j - M_j^T M_j D_j N_j - N_j D_j M_j^T M_j + N_j D_j M_j^T M_j D_j N_j. \tag{38}$$

From (12) it follows that

$$\hat{x}_s = [S_j^T \hat{M}_j^T \hat{M}_j S_j]^{-1} S_j^T \hat{M}_j^T \hat{M}_j \hat{\mu}_j. \tag{39}$$

We will approximate the expected value of the right-hand side of (39) by

$$E\{\hat{x}_s\} = [E\{S_j^T \hat{M}_j^T \hat{M}_j S_j\}]^{-1} E\{S_j^T \hat{M}_j^T \hat{M}_j \hat{\mu}_j\}. \tag{40}$$

This approximation is a good one when $S_j^T M_j^T M_j S_j$ is a well-conditioned matrix and the measurement noise is small. From (38) it follows that

$$H \triangleq E\{S_j^T \hat{M}_j^T \hat{M}_j S_j\} = S_j^T M_j^T M_j S_j + S_j^T\,\text{diag}\,\{D_j M_j^T M_j D_j\}\Sigma S_j. \tag{41}$$

Next note that

$$\hat{M}_j^T \hat{M}_j \hat{\mu}_j = M_j^T M_j \mu_j - \frac{1}{2} M_j^T M_j n_j \odot n_j + M_j^T M_j D_j N_j \rho_j \odot n_j + N_j D_j M_j^T \rho_j \odot n_j + N_j D_j M_j^T M_j D_j N_j \mu_j + \text{terms containing } n_j + \text{terms containing 3rd and 4th powers of } n_j. \tag{42}$$

Taking the expected value of (42) will eliminate the terms containing n_j, and higher order terms are neglected. Thus

$$K \triangleq E\{\hat{M}_j^T \hat{M}_j \hat{\mu}_j\} = M_j^T M_j \mu_j - \frac{1}{2} M_j^T M_j \sigma^2 + M_j^T M_j \sigma^2 + \text{diag}\,\{D_j M_j^T M_j D_j^{-1}\}\sigma^2 + \text{diag}\,\{D_j M_j^T M_j D_j\}\sigma^2 \odot \mu_j. \tag{43}$$

It follows that

$$E\{\hat{x}_s\} = H^{-1} S_j^T K. \tag{44}$$

Since $\hat{x}_s = x_s + \tilde{x}_s$, we get

$$\text{BIAS} = E\{\tilde{x}_s\} = H^{-1} S_j K - x_s. \tag{45}$$

Accuracy Optimization

In the discussion so far the location equation (11), or equivalently (20), was assumed to be solved by a standard least squares technique. It is possible, of course, to use instead a *weighted* least squares procedure. Let W be a positive definite $(N-2) \times (N-2)$ weighting matrix and premultiply (20) by $W^{1/2}$ to yield the weighted version of the location estimator:

$$W^{1/2} \bar{M}_j x_s = W^{1/2} \bar{M}_j \mu_j \tag{46a}$$

or

$$x_s = (S_j^T \bar{M}_j^T W \bar{M}_j S_j)^{-1} S_j^T \bar{M}_j^T W \bar{M}_j \mu_j. \tag{46b}$$

The covariance and bias of this estimator are obtained by replacing M_j with $W^{1/2}\bar{M}_j$ in (27) and (34) or (35).

The question naturally arises as to what choice of the weighting matrix W will lead to the best possible accuracy. To answer this question we will first rewrite the covariance equation (27) for the weighted case as

$$\text{COV}_W\{\tilde{x}_s\} = (A^T W A)^{-1} A^T W C W A (A^T W A)^{-1} \tag{47a}$$

where

$$A = \bar{M}_j S_j \tag{47b}$$

$$C = \bar{M}_j\,(\text{diag}\,\{\rho_j\} + R_{js} I)\Sigma\,(\text{diag}\,\{\rho_j\} + R_{js} I) M_j^T. \tag{47c}$$

Next we show that

$$W^* = C^{-1} \tag{48}$$

is the optimal weighting matrix in the sense that

$$\text{COV}_W\{\tilde{x}_s\} \geq \text{COV}_{W^*}\{\tilde{x}_s\} = (A^T C^{-1} A)^{-1} \tag{49}$$

for all permissible choices of W. The proof consists of verifying that

$$\text{COV}_W\{\tilde{x}_s\} - \text{COV}_{W^*}\{\tilde{x}_s\} = [(A^T W A)^{-1} A^T W - (A^T C^{-1} A)^{-1} A^T C^{-1}] \cdot C[(A^T W A)^{-1} A^T W - (A^T C^{-1} A)^{-1} A^T C^{-1}]^T. \tag{50}$$

Since $C > 0$ the right-hand side of (50) is clearly nonnegative definite and (49) immediately follows.

Note that the derivation above requires that C and, therefore, $\bar{M}_j$ be nonsingular. This is the reason we used (20) rather than (11) in the development above (i.e., $\bar{M}_j$ is nonsingular, while M_j is singular).

The optimal weighting matrix is dependent on the RD's and on R_{js} (which can be computed from the RD's via (15)). In a practical situation we will replace the measured RD's into (48) which results in an estimate $\hat{W}^*$ of the optimal weighting

matrix. Using the estimate $\hat{W}^*$ rather than W^* can be shown to have a relatively small effect on the resulting accuracy.

The Variance and Bias in Rotated Coordinates

The error covariance matrix defines an "uncertainty ellipse." As we will see in Section VI, this ellipse is typically highly eccentric (i.e., its major axis is much larger than its minor axis). Therefore, it is of interest to display the variance and bias in the directions of these axes, rather than the prespecified (x, y) coordinates. Next we derive the necessary coordinate rotation.

Let

$$\text{COV}\ \{\tilde{x}_s\} = \bar{U}\bar{\Sigma}\bar{U}^T$$

be the singular value decomposition of the error covariance matrix, where

$$\bar{U} = \begin{bmatrix} \cos\theta & -\sin\theta \\ \sin\theta & \cos\theta \end{bmatrix}$$

is a rotation matrix, and where

$$\bar{\Sigma} = \begin{bmatrix} \bar{\sigma}_{\tilde{x}}^2 & 0 \\ 0 & \bar{\sigma}_{\tilde{y}}^2 \end{bmatrix}.$$

The angle θ gives the orientation of the major axis of the uncertainty ellipse, $\bar{\sigma}_1$ is the standard deviation of the error in the major axis direction, while $\bar{\sigma}_2$ is the standard deviation of the error in the minor axis direction.

Finally, the bias in the rotated coordinates is given by

$$\begin{bmatrix} \bar{x} \\ \bar{y} \end{bmatrix} = \bar{U}^T E\{\tilde{x}_s\}.$$

In the case where the source is far from the sensors (compared to the maximum sensor separation), the major axis of the uncertainty ellipse is along the line connecting the sensors to the source, while the minor axis is perpendicular to that line. In other words, a small array or cluster of sensors provides relatively poor range estimation, while it is capable of providing good bearing estimation. In the case of a source located near or inside a cluster of sensors, the notions of range and bearing are not well defined, and it is not obvious how the uncertainty ellipse will be oriented. The formulas derived in this section provide the answer.

IV. Localization in the Case of a Minimal Number of Sensors

The localization algorithm presented in Section II requires that the number of sensors exceed the minimal number $(n + 1)$ required to solve the problem. A question of considerable practical interest is how to localize the source when only the minimal number of sensors $(N = n + 1)$ is available. In this section we derive an explicit formula for the source location for this case.

Consider the two-dimensional case $(n = 2)$ with the first sensor being the reference sensor $(j = 1)$. Equation (11) reduces in this case to

$$[r_{31}(x_2 - x_1) - r_{21}(x_3 - x_1)]x_s + [r_{31}(y_2 - y_1) - r_{21}(y_3 - y_1)]y_s = r_{31}m_1 - r_{21}m_2 \quad (51a)$$

where

$$m_i = \frac{1}{2}(R_{io}^2 - R_{1o}^2 - r_{i1}^2), \qquad i = 1, 2 \quad (51b)$$

are the elements of μ_j.

Equation (51) can be rewritten as

$$y_s = \alpha x_s + \beta \quad (52a)$$

where

$$\alpha = \frac{r_{21}(x_3 - x_1) - r_{31}(x_2 - x_1)}{-r_{21}(y_3 - y_1) + r_{31}(y_2 - y_1)} \quad (52b)$$

$$\beta = \frac{r_{31}m_1 - r_{21}m_2}{-r_{21}(y_3 - y_1) + r_{31}(y_2 - y_1)}. \quad (52c)$$

As may be expected, (11) establishes a single straight LOP for the source coordinates. In order to pinpoint the source location along the LOP we use the first of two equations in (7a):

$$(x_2 - x_1)x_s + (y_2 - y_1)y_s = m_1 - R_{1s}r_{21}. \quad (53)$$

Inserting (52) into (53) and rearranging terms we get

$$R_{1s} = \frac{1}{r_{21}}\{[(x_2 - x_1) + (y_2 - y_1)\alpha]x_s + (y_2 - y_1)\beta - m_1\}. \quad (54)$$

Note also that

$$\begin{aligned} R_{1s} &= [(x_1 - x_s)^2 + (y_1 - y_s)^2]^{1/2} \\ &= [(x_1 - x_s)^2 + (y_1 - \alpha x_s - \beta)^2]^{1/2} \\ &= [(1 + \alpha^2)x_s - 2(x_1 + (y_1 - \beta)\alpha)x_s \\ &\quad + (y_1 - \beta)^2 + x_1^2]^{1/2}. \end{aligned} \quad (55)$$

Squaring (54) and (55) and equating their left-hand sides gives a quadratic equation for x_s

$$\gamma_2 x_s^2 + \gamma_1 x_s + \gamma_o = 0 \quad (56a)$$

where

$$\gamma_2 + 1\alpha^2 - \{[(x_2 - x_1) + (y_2 - y_1)\alpha]/r_{21}\}^2 \quad (56b)$$

$$\gamma_1 = -2\{x_1 + (y_1 - \beta)\alpha + [(x_2 - x_1) + (y_2 - y_1)\alpha][(y_2 - y_1)\beta - m_1]/r_{21}^2\} \quad (56c)$$

$$\gamma_0 = x_1^2 - \{[(y_2 - y_1)\beta - m_1]/r_{21}\}^2. \quad (56d)$$

Thus the explicit formula for the source coordinates is

$$x_s = [-\gamma_1 \pm \sqrt{\gamma_1^2 - 4\gamma_0\gamma_2}]/(2\gamma_2) \quad (57a)$$

$$y_s = \alpha x_s + \beta. \quad (57b)$$

An error analysis of these estimates can be carried out by expanding (x_s, y_s) in a first-order Taylor expansion around the true values of r_{21}, r_{31}:

$$\begin{bmatrix} \tilde{x}_s \\ \tilde{y}_s \end{bmatrix} = \underbrace{\begin{bmatrix} \frac{\partial x_s}{\partial r_{21}} & \frac{\partial x_s}{\partial r_{31}} \\ \frac{\partial y_s}{\partial r_{21}} & \frac{\partial y_s}{\partial r_{31}} \end{bmatrix}}_{G} \begin{bmatrix} n_1 \\ n_2 \end{bmatrix} \quad (58)$$

where n_1, n_2 are the measurement errors corresponding to r_{21} and r_{31}. Thus

$$\text{COV}\ \{\tilde{x}_s\} = G\Sigma G^T. \tag{59}$$

The explicit form of G is given in [12]. The bias term can be evaluated by a second-order Taylor expansion [12].

A very similar procedure can be applied in the three-dimensional case ($n = 3$) to derive explicit formulas for the source coordinates (x_s, y_s, z_s) and to analyze their accuracy properties. Equation (11) reduces in this case to

$$\underbrace{[r_{31}(x_2-x_1)-r_{21}(x_3-x_1)]}_{A_1}x_s+\underbrace{[r_{31}(y_2-y_1)-r_{21}(y_3-y_1)]}_{B_1}y_s$$
$$+\underbrace{[r_{31}(z_2-z_1)-r_{21}(z_3-z_1)]}_{C_1}z_s=\underbrace{r_{31}m_1-r_{21}m_2}_{D_1} \tag{59a}$$

$$\underbrace{[r_{41}(x_3-x_1)-r_{31}(x_4-x_1)]}_{A_2}x_s+\underbrace{[r_{41}(y_3-y_1)-r_{31}(y_4-y_1)]}_{B_2}y_s$$
$$+\underbrace{[r_{41}(z_3-z_1)-r_{31}(z_4-z_1)]}_{C_2}z_s=\underbrace{r_{41}m_2-r_{31}m_3}_{D_2}.$$

Multiplying the two equations above by C_3 and C_2, respectively, and subtracting, we get

$$(A_1C_2-A_2C_1)x_s+(B_1C_2-B_2C_1)y_s=D_1C_2-D_2C_1$$

or

$$y_s=\alpha_1x_s+\beta_1 \tag{59b}$$

where

$$\alpha_1=(A_1C_2-A_2C_1)/(B_1C_2-B_2C_1)$$
$$\beta_1=(D_1C_2-D_2C_1)/(B_1C_2-B_2C_1). \tag{59c}$$

Substituting (59b) in (59a), we get

$$(A_1+\alpha_1B_1)x_s+C_1z_s=D_1-B_1\beta_1$$

or

$$z_s=\alpha_2x_s+\beta_2$$
$$\alpha_2=-(A_1+\alpha_1B_1)/C_1$$
$$\beta_2=(D_1-B_1\beta_1)/C_1. \tag{59d}$$

Thus (11) yields a single straight LOP for the source location. In order to pinpoint the source location along the LOP, we use the first row of (7a)

$$(x_2-x_1)x_s+(y_2-y_1)y_s+(z_2-z_1)z_s=m_1-R_{1s}r_{21}. \tag{59e}$$

Inserting (59c) and (59d) into (59e) and rearranging terms, we get

$$R_{1s}=-\frac{1}{r_{21}}[(x_2-x_1)+\alpha_1(y_2-y_1)+\alpha_2(z_2-z_1)]x_s$$
$$+\frac{1}{r_{21}}[m_1-(y_2-y_1)\beta_1-(z_2-z_1)\beta_2]=\alpha_3x_s+\beta_3. \tag{59f}$$

Note also that

$$R_{1s}=[(x_1-x_s)^2+(y_1-y_s)^2+(z_1-z_s)^2]^{1/2}$$
$$=[(1+\alpha_1^2+\alpha_2^2)x_s^2-2(x_1+(y_1-\beta_1)\alpha_1+(z_1-\beta_2)\alpha_2)x_s$$
$$+(y_1-\beta_1)^2+(z_1-\beta_2)^2+x_1^2]^{1/2}. \tag{59g}$$

Squaring up (59f) and (59g) and equating terms leads to a quadratic equation for x_s:

$$\underbrace{(1+\alpha_1^2+\alpha_2^2-\alpha_3^2)}_{\gamma_2}x_s^2$$
$$-\underbrace{2(x_1+(y_1-\beta_1)\alpha_1+(z_1-\beta_1)\alpha_2+\alpha_3\beta_3)}_{\gamma_1}x_s$$
$$+\underbrace{[(y_1-\beta_1)^2+(z_1-\beta_2)^2+x_1^2-\beta_3^2]}_{\gamma_0}=0$$

and therefore

$$x_s=[-\gamma_1\pm\sqrt{\gamma_1^2-4\gamma_0\gamma_2}]/(2\gamma_2)$$
$$y_s=\alpha_1x_s+\beta_1$$
$$z_s=\alpha_2x_s+\beta_2.$$

An error analysis of the resulting estimates follows the same steps as in the two-dimensional case [cf. the discussion surrounding (58)]: see [12].

V. Velocity Estimation from Range and Range-rate Differences

In this section we derive an algorithm for estimating the velocity of a moving source when measurements of range-rate differences are available in addition to the range difference measurements considered in earlier sections. In other words, given noisy measurements of $\{r_{ij}, \dot{r}_{ij}, i, j = 1, \cdots, N\}$ where $\dot{r}_{ij} \triangleq \partial r_{ij}/\partial t$, we wish to estimate the source velocity vector $\dot{\boldsymbol{x}}_s \triangleq \partial \boldsymbol{x}_s/\partial t$. As was mentioned before, range-rate measurements are available in situations where the Doppler shifts of signals emanating from the target can be estimated.

The basic equations for the source velocity are obtained by differentiating (7a) with respect to time:

$$S_j\dot{\boldsymbol{x}}_s=\dot{\boldsymbol{\mu}}_j-\dot{R}_{js}\boldsymbol{\rho}_j-R_{js}\dot{\boldsymbol{\rho}}_j$$
$$=\underbrace{[\text{diag}\ \{\boldsymbol{\rho}_j\}-R_{js}I]}_{Q_j}\dot{\boldsymbol{\rho}}_j-\dot{R}_{js}\boldsymbol{\rho}_j \tag{60}$$

where $\boldsymbol{\rho}_j$ is the vector of range differences (see (7d)) and $\dot{\boldsymbol{\rho}}_j$ is the vector or range-rate differences, similarly defined.

As in Section II, we eliminate the term $\boldsymbol{\rho}_j$ on the right-hand side by premultiplying (60) by M_j (see (8)). Thus the source velocity vector is given by the least squares solution of the following set of $(N-1)$ linear equations:

$$M_jS_j\dot{\boldsymbol{x}}_s=M_jQ_j\dot{\boldsymbol{\rho}}_j \tag{61}$$

or

$$\dot{\boldsymbol{x}}_s=(S_j^TM_j^TM_jS_j)^{-1}S_j^TM_j^TM_jQ_j\dot{\boldsymbol{\rho}}_j. \tag{62}$$

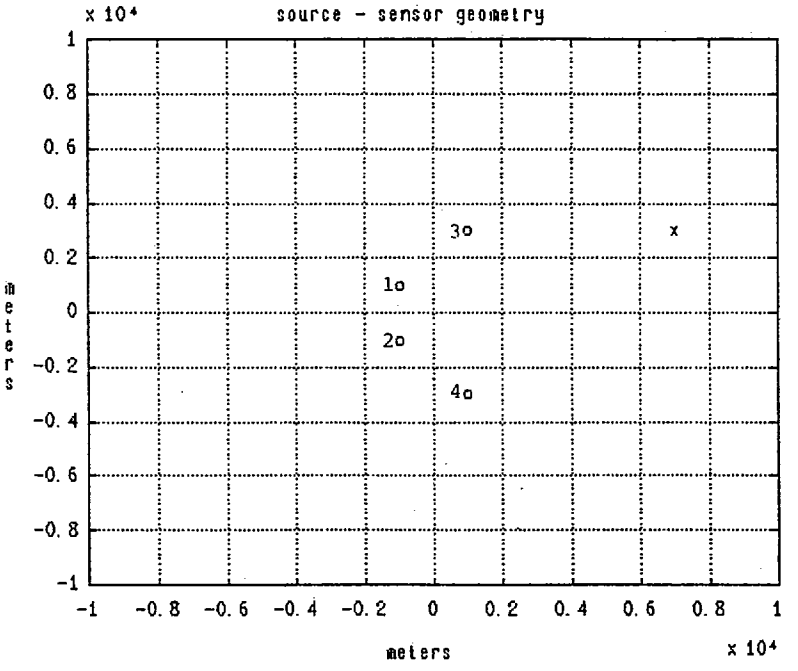

Fig. 4. The source-sensor geometry, four-sensor case.

Note that Q_j, M_j are determined from the range-difference measurements. To evaluate R_{js}, which is needed for Q_j, we solve for x_s using (11) or (20) and set $R_{js} = \|x_j - x_s\|$. An alternative set of $(N - 2)$ linear equations is obtained by replacing M_j in (61) by M_j (see (19)).

The analysis of the accuracy of the velocity estimates is straightforward, provided that we assume that the errors in measuring $\{r_{ij}\}$ and $\{\dot{r}_{ij}\}$ are mutually uncorrelated.

Let Σ_r and $\Sigma_{\dot{r}}$ denote the covariance matrices of the measurement noise processes n_r and $n_{\dot{r}}$ corresponding to ρ_j and $\dot{\rho}_j$, respectively. It follows from (60) that

$$M_j S_j \hat{\dot{x}}_s = M_j(Q_j + \text{diag}\,\{n_r\})(\dot{\rho}_j + n_{\dot{r}}). \tag{63}$$

As before, we ignore the randomness in $\hat{M}_j$ and replace it by its true value M_j. From (63) we get

$$M_j S_j \hat{\dot{x}}_s = M_j(n_r \odot \dot{\rho}_j + Q_j n_{\dot{r}} + n_r \odot n_{\dot{r}})$$

and

$$M_j S_j \text{ COV } \{\tilde{\dot{x}}_s\} S_j^T M_j^T = M_j\,(\text{diag}\,\{\dot{\rho}_j\}\Sigma_r \text{ diag}\,\{\dot{\rho}_j\} + Q_j \Sigma_{\dot{r}} Q_j^T + \Sigma_r \Sigma_{\dot{r}}) M_j^T.$$

Thus

$$\text{COV}\,\{\tilde{\dot{x}}_s\} = H_j L_j H_j^T$$

where

$$H_j = (S_j^T M_j^T M_j S_j)^{-1} S_j^T M_j^T M_j$$

$$L_j = \text{diag}\,\{\dot{\rho}_j\}\Sigma_r \text{ diag}\,\{\dot{\rho}_j\} + Q_j \Sigma_{\dot{r}} Q_j^T + \Sigma_r \Sigma_{\dot{r}}.$$

The bias of the velocity estimator can be analyzed using the same procedures employed in Section III for evaluating the bias of the location vector. We defer the details to [12].

We note that a problem of considerable practical interest is to localize a source from measurement of range-rate differences only (i.e., $\dot{r}_{ij}$ is measured, but not r_{js}). The estimation of the source location is considerably more complicated and it does not seem possible to obtain a linear equation formulation in this case. However, some practical solution methods are available (see [12]).

VI. Numerical Examples

The performance of the proposed location estimation algorithm was evaluated by extensive Monte-Carlo simulations. In this section we present a few selected examples to illustrate the validity of the analytical expressions for the covariance and bias of the estimates, and the effect of optimal weighting.

Three different sensor configurations were used: a four-sensor cluster depicted in Fig. 4, a six-sensor cluster depicted in Fig. 5, and an eight-sensor configuration depicted in Fig. 6. Sensor number 1 was the reference sensor. The target coordinates were (7000, 3000) in all cases (all location-related parameters are specified in meters). Zero-mean Gaussian noise was added to the range differences with variance chosen so that all sensors have the same signal-to-noise ratio (SNR). The variance of the noise added to the ith sensor was $\sigma \cdot |r_{i1}|$, resulting in SNR $= 1/\sigma^2$ for all sensors.

Table I summarizes the theoretical and sample statistics for $(\hat{x}_s, \hat{y}_s)$ obtained by 500 independent Monte-Carlo sums. The mean-square error was computed in addition to the mean and standard deviation (mse $= [\text{mean}^2 + \text{std}^2]^{1/2}$).

The location estimates were computed by solving (11) with $M_{nw} = (I - Z)D$ (cf. (8)) in the nonweighted case and $M_w = W^{1/2}\bar{M}_j$ (cf. (19), (46)) in the weighted case. The theoretical covariance was computed using (27) with M_{nw} and M_w as defined above. The bias was computed from (35) in the four-

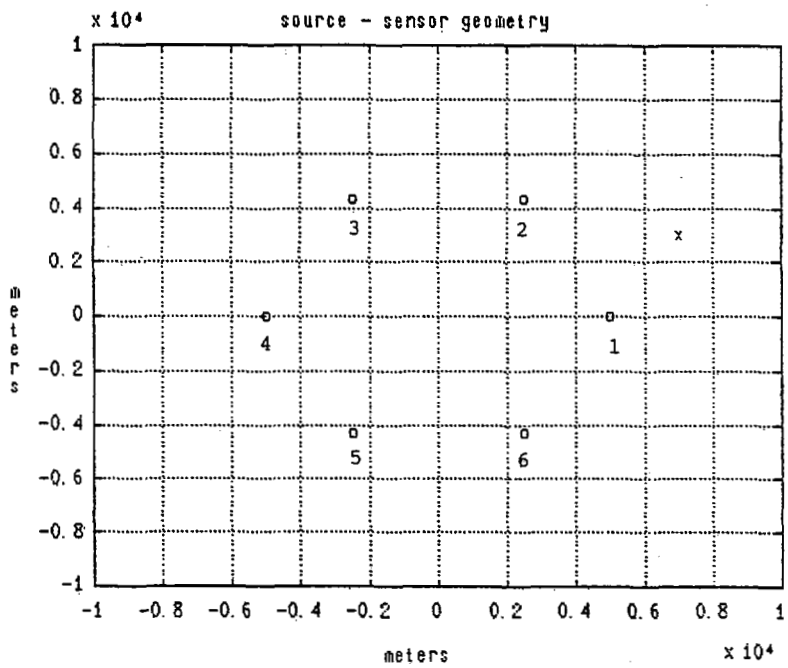

Fig. 5. The source-sensor geometry, six-sensor case.

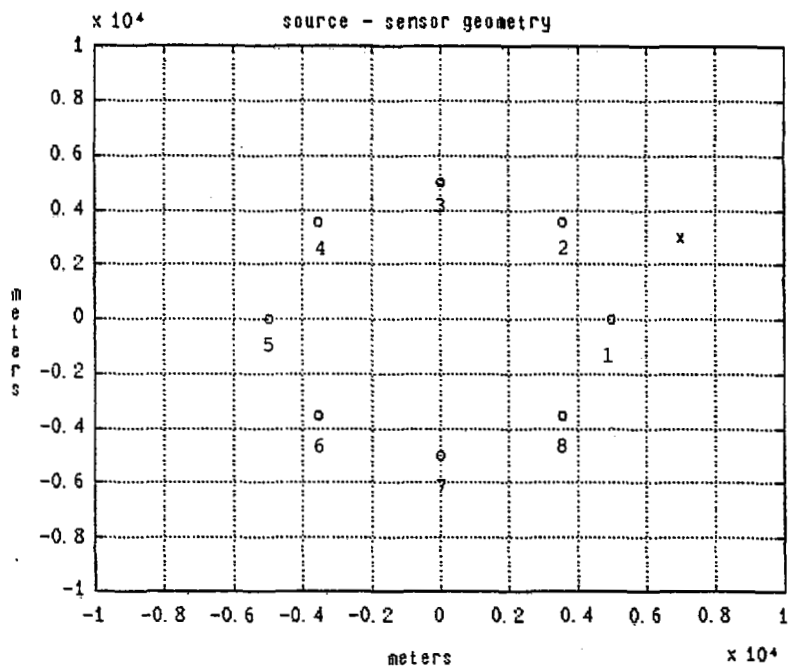

Fig. 6. Source-sensor geometry for the eight-sensor case.

sensor case and from (45) in the six- and eight-sensor cases, with M_{nw}, M_w as above. In the four-sensor case, the weighted and unweighted estimates are identical. Therefore, results for the weighted case are given only for the six- and eight-sensor cases. The mean and standard deviations are also presented in rotated coordinates with θ being the angle of rotation.

The following observations can be made from Table I, and from other simulations not reported here.

a) There is excellent agreement between the sample and theoretical variances of the estimates.

b) In the four-sensor case the theoretical values of the bias from (35) are very close to the sample mean. The bias computed from (35) differed significantly from the sample mean when more than four sensors were used.

c) In the six-sensor case the bias from (45) often exceeded the sample mean by a significant amount, but predicted correctly its sign and order of magnitude. In test cases with a larger number of sensors the bias computed from (45) was much closer to the sample mean.

d) The optimally weighted estimates were always more accurate than the nonweighted estimates, but the difference was quite small and not practically significant.

TABLE I
ERROR STATISTICS FOR THE LOCATION ESTIMATES ($\hat{x}_s$, $\hat{y}_s$) AND THE ROTATED ESTIMATES $\{\bar{x}, \bar{y}\}$

		$\hat{x}_s$			$\hat{y}_s$			$\theta°$	$\bar{x}$		$\bar{y}$	
		mean	std.	mse.	mean	std.	mse.		mean	std.	mean	std.
4 sensors	theory	0.3037	39.58	39.58	.1794	23.27	23.27	30.45	.3528	45.91	.0007	.5532
$\sigma = .001$	simulation	0.2983	39.33	39.33	.1758	23.07	23.07	30.38	.3462	.4560	.0008	.5820
4 sensors	theory	30.37	395.8	397.0	17.94	232.7	233.4	30.45	35.28	459.1	.0728	5.532
$\sigma = .01$	simulation	30.26	401.1	402.3	17.83	235.3	236.0	38.85	35.12	465.0	.0765	5.861
6 sensors	theory	-.8331	40.11	40.12	-.2965	13.65	13.66	18.69	-.8892	42.34	-.0139	1.572
$\sigma = .001$	simulation	-.4215	41.30	41.31	-.1534	14.16	14.16	18.83	-.4484	43.64	-.0091	1.550
6 sensors	theory	-82.62	401.1	409.6	-29.41	156.5	159.7	18.69	-87.68	423.4	-1.379	15.72
$\sigma = .01$	simulation	-42.01	415.3	415.5	-15.29	141.8	142.6	18.84	-44.70	436.7	-.9024	15.47
8 sensors	theory	-.8969	25.46	25.47	-0.3912	11.20	11.20	23.75	-.9785	27.81	.0031	.1353
$\sigma = .001$	simulation	-.7126	25.58	25.59	-0.3105	11.24	11.25	23.73	-.7773	27.93	.0026	.1375
8 sensors	theory	-88.89	254.6	269.6	-38.78	112.6	118.5	23.75	-96.98	278.1	.3068	1.353
$\sigma = .01$	simulation	-70.59	259.9	269.3	-30.76	114.2	118.3	23.73	-77.00	283.9	.2461	1.374
optimally weighted												
6 sensors	theory	-.6211	37.93	37.94	-.2113	13.02	13.02	18.83	-.6561	40.07	.0006	1.541
$\sigma = .001$	simulation	-.1486	38.72	38.72	-.0503	13.37	13.37	18.94	-.4484	40.93	-.0082	1.538
6 sensors	theory	-61.67	379.3	384.3	-20.98	150.2	151.9	18.83	-65.14	400.77	.0557	15.41
$\sigma = .01$	simulation	-14.91	387.0	387.3	-5.053	153.6	153.7	18.94	-44.70	409.1	-.8204	15.35
8 sensors	theory	-.4299	25.29	25.30	-.1891	11.13	11.13	23.75	-.4696	27.63	.0000	.1341
$\sigma = .001$	simulation	-.1908	25.69	25.69	-.0839	11.30	11.30	23.73	-.7773	28.06	.0026	.1366
8 sensors	theory	-42.76	252.9	256.5	-18.81	111.3	112.9	23.74	-46.71	276.3	-.0012	1.341
$\sigma = .01$	simulation	-19.06	256.8	257.5	-8.382	112.9	113.2	23.73	-77.00	280.5	.2556	1.365

TABLE II
LOCALIZATION FOR DIFFERENT CHOICES OF THE REFERENCE SENSOR

reference sensor location	theoretical std. unweighted case		theoretical std. weighted case		theoretical std. unweighted case			theoretical std. weighted case		
	$\hat{x}_s$	$\hat{y}_s$	$\hat{x}_s$	$\hat{y}_s$	$\theta°$	$\bar{x}$	$\bar{y}$	$\theta°$	$\bar{x}$	$\bar{y}$
(5000,0)	40.11	13.65	37.93	13.02	18.69	42.34	1.572	18.83	40.08	1.541
(2500,4330)	33.04	11.32	31.40	10.84	18.83	34.91	1.170	18.97	33.20	1.139
(-2500,4330)	16.48	7.038	13.90	6.105	22.95	17.89	1.019	23.53	15.15	.8955
(-5000,0)	19.24	9.090	18.17	8.561	25.20	21.26	.9300	25.13	20.06	.9100
(-2500,-4330)	17.43	8.085	16.59	7.670	24.77	19.20	.8902	24.71	18.26	.8668
(2500,-4330)	17.45	8.173	16.57	7.841	24.97	19.25	.9633	25.22	18.31	.8668

e) The bias was always small compared to the standard deviation. Thus localization accuracy was dominated by the variance of the estimator.

f) The uncertainty ellipse was highly eccentric in all test cases, with the ratio of its axes being on the order of 50–200.

g) As may be expected, the standard deviation is proportional to σ, while the bias is proportional to σ^2.

Next we consider the effect of choosing the reference sensor on localization accuracy. Table II summarizes the theoretical standard deviations of the estimator for the six-sensor case considered earlier, with $\sigma = 0.001$. These results were matched very closely by Monte-Carlo simulation results. The first reference sensor was the rightmost sensor in Fig. 6. The other sensors follow in a counterclockwise direction. From examination of Table II we note that choosing different reference sensors affects the accuracy by a considerable amount. Using the expressions developed in this paper, we can always choose the best reference sensor for any given situation. Note also that the orientation of the uncertainty is affected only slightly by the choice of the reference sensor.

VII. DISCUSSION

In this paper we developed a localization algorithm which requires solving a linear set of equations, and presented formulas for the covariance and bias of the resulting estimates. These formulas are very useful for performance prediction and for system design. Using these formulas, the sensor configuration can be optimized for best accuracy for a given surveillance scenario. Combining these results with formulas for the variance of the range-difference measurements, we obtain a measure of localization accuracy in terms of system parameters such as signal bandwidth, integration time, and sensor SNR. In the passive sonar problem, simple formulas are available to the asymptotic variance of the delay (range) estimates (see [13]).

Tracking algorithms for localization from range-difference measurements usually involves the use of the extended Kalman filter (EKF) due to the nonlinearity of the equations relating the measurements to the state vector. The formulation presented here leads to a *linear* set of equations making it possible to use a *linear* Kalman filter. For example, (11) may be interpreted as a linear (although data-dependent) measurement equation for the state vector $\boldsymbol{x}_s$ where $M_j S_j$ is the measurement matrix and $M_j \boldsymbol{\mu}_j$ is the "data vector." Replacing the EKF by a linear Kalman filter has several advantages: it is computationally simpler and it avoids some of the convergence problems often encountered in the EKF.

In our simulation study we found the localization algorithm

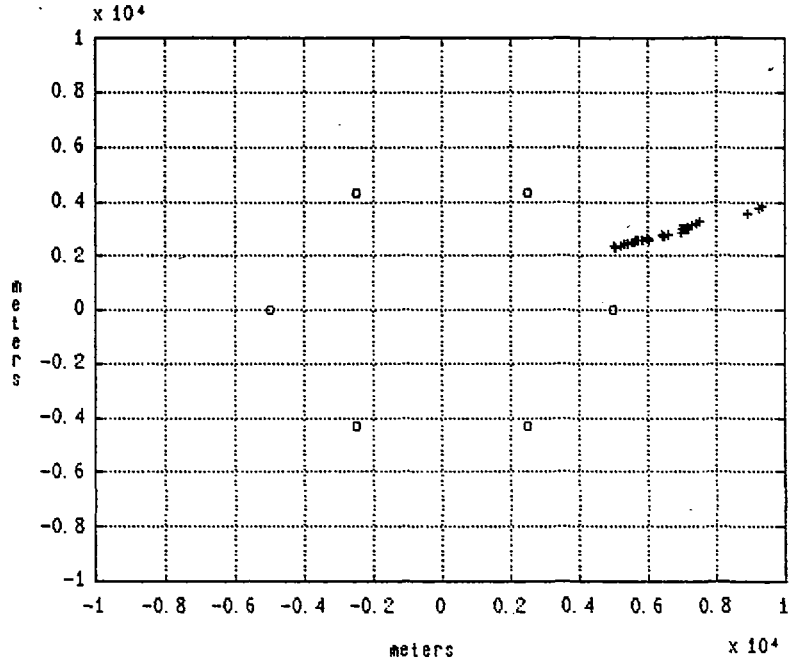

Fig. 7. The effect of bias in the range difference measurements.

to have a relatively small bias (compared to the standard deviation of the estimates). This observation is true only if the range-difference measurements are essentially unbiased. Any bias in the measurement translates into bias in the location estimate. Equations (7) and (12) can be used to study the sensitivity of the location estimate to bias in the range measurements.

This sensitivity is much greater in the direction of the major axis of the uncertainty ellipse than in the direction perpendicular to it. To study this effect we introduce deterministic errors of the form

$$n_j = \sigma \begin{bmatrix} \pm 1 \\ \pm 1 \\ \vdots \\ \pm 1 \end{bmatrix}$$

to the measurements $\{r_{ij}\}$ [cf. (22)]. For each choice of the error vector we compute a location estimate. A scatter plot of the $2^{(N-1)}$ location estimates obtained in this way provides a pictorial indication of the effects of bias. Fig. 7 presents this plot for the six-sensor case with $\sigma = 0.03$.

References

[1] R. O. Schmidt, "A new approach to geometry of range difference location," *IEEE Trans. Aerosp. Electron. Syst.*, vol. AES-8, no. 6, pp. 821–835, Nov. 1972.

[2] J. M. Delosme, M. Morf, and B. Friedlander, "Estimating source location from time-difference-of-arrival: A linear equation approach," Information Systems Lab., Stanford, CA, Tech. Rep. M355-1, Mar. 31, 1979.

[3] J. M. Delosme, M. Morf, and B. Friedlander, "A linear equation approach to locating sources from time-difference-of-arrival measurements," in *Proc. IEEE Int. Conf. Acoustics, Speech, and Signal Processing* (Denver, CO), 1980, pp. 818–824.

[4] J. S. Abel and J. O. Smith, "The spherical interpolation method to closed form passive source localization using range difference measurements," in *Proc. IEEE Int. Conf. Acoustics, Speech, Signal Processing* (Dallas, TX), 1987, pp. 471–474.

[5] J. J. Dongara, C. B. Moler, J. R. Bunch, and G. W. Stewart, *LINPACK User's Guide.* Philadelphia, PA: SIAM, 1979.

[6] G. Golub and C. Van Loan, *Matrix Computations.* Baltimore, MD: Johns Hopkins Univ. Press, 1984.

[7] J. L. Poirot and G. V. McWilliams, "Application of linear statistical models to radar location techniques," *IEEE Trans. Aerosp. Electron. Syst.*, vol. AES-10, no. 6, pp. 830–834, Nov. 1974.

[8] W. M. Foy, "Position-location solutions by Taylor series estimation," *IEEE Trans. Aerosp. Electron. Syst.*, vol. AES-12, no. 2, pp. 187–194, Mar. 1976.

[9] J. P. Van Etten, "Navigation systems: Fundamentals of low and very low frequency hyperbolic techniques," *Electrical Commun.*, vol. 45, no. 3, pp. 192–212, 1970.

[10] H. B. Lee, "A novel procedure for assessing the accuracy of hyperbolic multilateration systems," *IEEE Trans. Aerosp. Electron. Syst.*, vol. AES-11, no. 1, pp. 2–15, Jan. 1975.

[11] N. Marchand, "Error distributions of best estimate of position from multiple time difference hyperbolic networks," *IEEE Trans. Aerosp. Navig. Electron.*, vol. ANE-11, no. 2, pp. 96–100, June 1964.

[12] B. Friedlander, "Analysis of some passive localization algorithms," Saxpy Computer Corp., Sunnyvale, CA, Tech. Rep. 86-010, Mar. 10, 1986.

[13] B. Friedlander, "On the Cramer–Rao bound for Doppler and delay estimation," *IEEE Trans. Inform. Theory*, vol. IT-30, no. 3, pp. 575–580, May 1984.

★

Benjamin Friedlander (S'74–M'76–SM'82–F'87) was born on February 24, 1947. He received the B.Sc. and the M.Sc. degrees in electrical engineering from the Technion, Israel Institute of Technology in 1968 and 1972, respectively, and the Ph.D. degree in electrical engineering and the M.Sc. degree in statistics from Stanford University, Stanford, CA, in 1976.

From 1968 to 1972 he served in the Israel Defence Forces as an Electronic Engineer. From 1976 to 1985 he was at Systems Control Technology, Inc., Palo Alto, CA. He was responsible for a number of research and development projects in the areas of signal processing and control, and was the Manager of the Advanced Technology Division. During this period he was

also a Lecturer at Stanford University, teaching graduate courses on linear systems, nonlinear detection and estimation, and system identification. In November of 1985 he joined Saxpy Computer Corporation, Sunnyvale, CA, as the Director of Advanced Technology. He is responsible for the R&D activities of the company and for the development of signal processing applications for the MATRIX 1—a 1000-Mflop supercomputer. He has authored more than 170 publications in the areas of signal processing and estimation. His current interests include parallel and systolic processing architectures and their VLSI implementations, advanced processing techniques for underwater surveillance, high-resolution spectral analysis and array processing, adaptive filtering, radar and communication processing, detection tracking and localization of multiple targets, image processing, and knowledge-based signal processing.

Dr. Friedlander was an Associate Editor of the *IEEE Transactions on Automatic Control* in 1984, a member of the Editorial Board of the *International Journal of Adoptive Control and Signal Processing*, and is a member of the Administrative Committee of the IEEE Acoustics, Speech, and Signal Processing (ASSP) Society. He serves as a member of the Technical Committee on Spectrum Estimation of the ASSP, and is the Vice-Chairman of the Bay Area Chapter of that society. He is a member of the IEEE Admission and Advancement Committee. He is the recipient of the 1983 ASSP Senior Award for the paper "Recursive Lattice Forms for Spectral Estimation," and the 1985 award for best paper of the year from the European Association for Signal Processing for the paper "On the Computation of an Asymptotic Bound for Estimating Autoregressive Signals in White Noise." He is a member of Sigma Xi.